

# Macrocyclic Schiff base Ligand and their Metal Complexes: Synthesis, characterization and biological studies

Haj Hasan Manal<sup>1\*</sup>, Al-khuder Mohammad Moudar<sup>1</sup> and Alkhuder Omar<sup>1,2</sup>

1. Department of Chemistry, Faculty of Science, Al-Baath University, Homs, SYRIA

2. Institute of Chemistry, St. Petersburg State University, St. Petersburg, RUSSIA

\*manalhajhasan75@gmail.com

## Abstract

The synthesis of a new ligand, *N*<sub>4</sub> Tetra (Methyl Azometine)-Di Phenyl hydrazide (TMADPH), was carried out by condensing 1,2-diacetylhydrazine with 1,4-phenylenediamin to obtain the ligand TMADPH. After confirming the structure of the bond using FT-IR, UV-VIS, <sup>1</sup>H-NMR and <sup>13</sup>C-NMR, its metal complexes with Zr<sup>4+</sup>, Mn<sup>2+</sup> and Ni<sup>2+</sup> were prepared and studied using FT-IR, UV-VIS spectroscopy, electrical conductivity and metal ratio analysis.

The results indicated that all the metal complexes had a mononuclear structure. Furthermore, the biological activity against *Pseudomonas aeruginosa* and *Staphylococcus aureus* bacteria was studied, revealing that the prepared metal complexes exhibited greater biological activity than the macrocyclic ligand.

**Keywords:** Macrocyclic ligand, 1, 2-Diacetylhydrazine, 1, 4-Phenylenediamin. Schiff bases ligand, Schiff bases complexes.

## Introduction

The chemistry of macrocycles and their metal complexes has garnered significant attention, evolving into an expanding field of research due to their exceptional applications in biology, supramolecular chemistry and the development of new materials<sup>3,12</sup>. The interest in macrocyclic complexes, particularly those with polydentate ligands, largely arises from the unique chemical properties that macrocyclic ligands confer upon these complexes. Additionally, the diverse geometric configurations and the potential encapsulation of metal ions within the rings contribute to their appeal<sup>6</sup>. Macrocyclic ligands play a crucial role in bioinorganic chemistry, catalysis, metal ion extraction from solutions and various other applications. Macrocyclic complexes with transition metal ions exhibit intriguing properties and biological functions including their role as models for metalloproteins and oxygen carrier systems<sup>7</sup>.

Structural factors, such as ligand rigidity and the type and arrangement of donor atoms, are crucial in determining the binding characteristics of macrocyclic ligands toward metal ions<sup>10</sup>. Macrocyclic Schiff bases have been extensively studied for their selective chelation of specific metal ions depending on the number, type and position of their donor

atoms, the metal ion's ionic radius and the coordinating properties of counterions<sup>2</sup>. These complexes are particularly important due to their resemblance to naturally occurring macrocycles, such as porphyrins (including hemoglobin, myoglobin, cytochromes and chlorophylls), cobalamins, corrins (like vitamin B12) and antibiotics (such as valinomycin and nonactin)<sup>9,14,17,18</sup>.

Cyclic and macrocyclic transition metal complexes are of significant interest for their application as diagnostic agents in magnetic resonance imaging. Macrocyclic molecules have profoundly influenced the fields of chemistry, biology and medicine<sup>5,11,13</sup> and are renowned for their anticancer, antibacterial and antifungal properties<sup>4,16</sup>. In this study, we aim to prepare Zr(IV), Mn(II) and Ni(II) complexes with the new macrocyclic ligand tetra (Methyl Azometine)-Di Phenyl hydrazide (TMADPH).

## Material and Methods

**Materials and Apparatus:** All chemicals used in this work were purchased from BDH, Aldrich and Merck companies and were used without further purification. NMR spectra were recorded on a Bruker instrument (400 MHz) spectrometer. Chemical shifts were reported in (δ) ppm relative to tetramethylsilane (TMS). Data were reported as follows: chemical shift, multiplicity, coupling constant (Hz), integration and assignment. FT-IR spectra (v, cm<sup>-1</sup>) were recorded on a JASCO Spectrum (FT-IR 4100) spectrometer using KBr pellets. UV-Vis spectroscopy was measured using a Jasco-V630-UV-Vis at the wavelength range of 200–1000 nm, using matched quartz cells (1 cm) and DMSO as the solvent.

**Synthesis of the ligand Tetra (Methyl Azometine)-Di Phenyl hydrazide (TMADPH):** A hot methanolic solution (60 ml) of 1,2-diacetylhydrazine (0.327 g, 2 mmol) and a methanolic solution (60 ml) of 1,4-phenylenediamine (0.220 g, 2 mmol) were mixed slowly under constant stirring. This mixture was refluxed at 65°C for 48 hours in the presence of a few drops of concentrated HCl (the pH was 6). Upon cooling, a brown-colored compound precipitated out. This was filtered, washed with hot methanol and dried under vacuum over P<sub>2</sub>O<sub>5</sub>. Yield: ≈ 56.732 %; M.P. 160°C. The preparation structural formula of the ligand are shown in fig. 1.

**Synthesis of [Zr(TMADPH)Cl<sub>2</sub>]·Cl<sub>2</sub> Cl<sub>2</sub> complex:** 0.188 g, 0.5 mmol was dissolved in 20 ml of methanol in a clean two-necked round bottom flask (250 mL) equipped with a

\* Author for Correspondence

magnetic stirrer and reflux condenser.  $ZrCl_4$  (0.116g, 0.5mmol) was added drop by drop to the ligand solution. The pH was adjusted to 11 using KOH and the mixture was then stirred at 65°C for 21 hours. The resulting precipitate was filtered, washed with methanol and then diethyl ether, dried and weighed. The melting point was determined as >300°C. Electrical conductivity was measured for the metal

complexes and it was 169  $\mu$ s, leading to the conclusion that the prepared metal complex was an electrolyte. Silver nitrate solution was used as an indicator for the determination of chloride ions, showing that the chloride ions were linked with metal ions in the coordination sphere. Metallic calculations indicated that the complex was monometallic. The structural formula of the complex is shown in fig. 2.

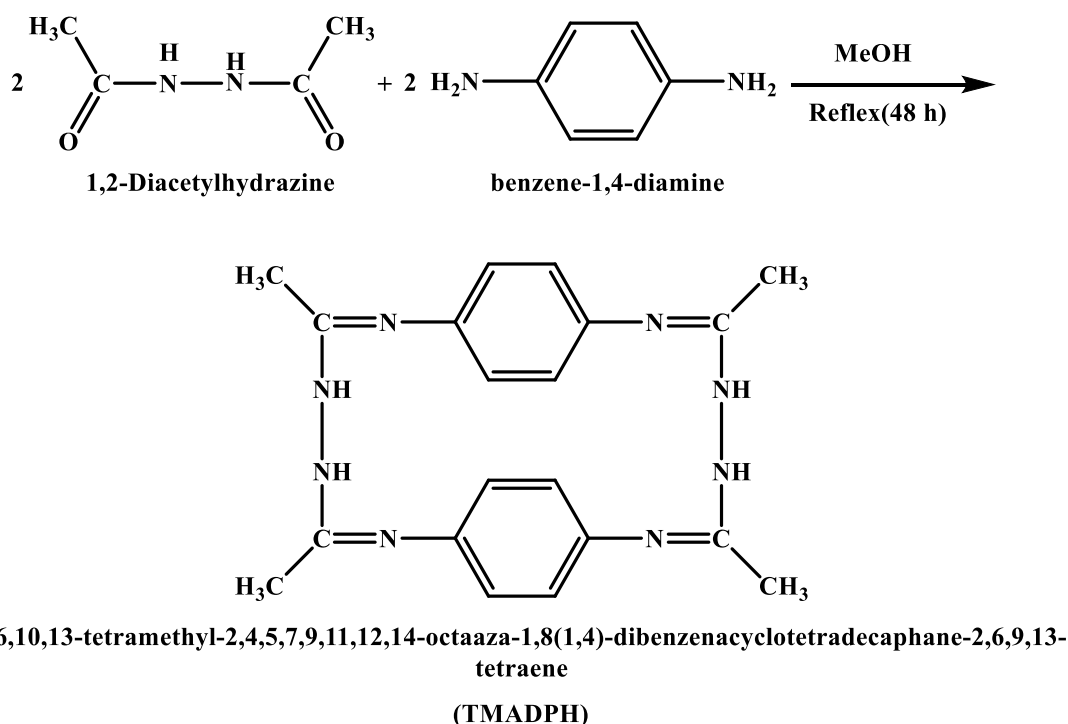


**Fig. 1: Preparation and structural formula of the ligand**

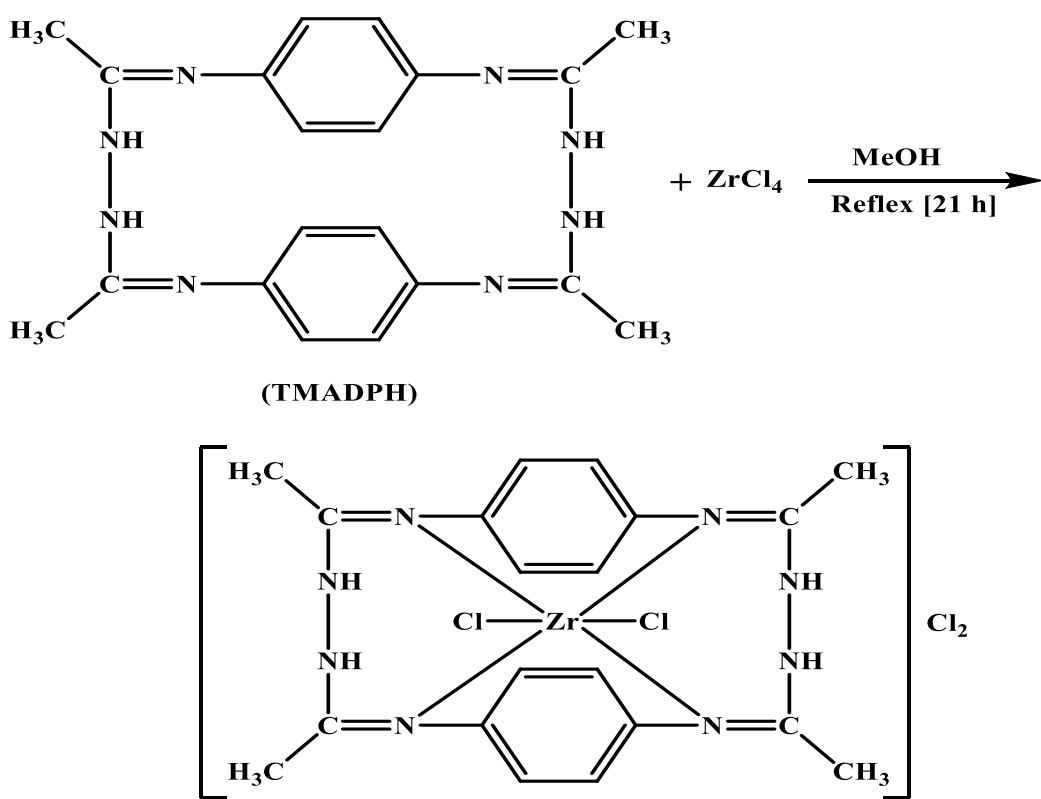


**Fig. 2: The structural formula of the metal complex**

**Synthesis of  $[\text{Mn}(\text{TMADPH})]\cdot\text{Cl}_2$  complex:** 0.188 g, 0.5 mmol was dissolved in 20 ml of methanol in a clean two-necked round bottom flask (250 mL) equipped with a magnetic stirrer and reflux condenser.  $\text{MnCl}_2$  (0.064 g, 0.5mmol) was added drop by drop to the ligand solution. The pH was adjusted to 11 using KOH and the mixture was then stirred at 65°C for 18 hours. The resulting precipitate was filtered, washed with methanol and then diethyl ether, dried and weighed. The melting point was determined as >300°C. Electrical conductivity was measured for the metal complexes and it was 145  $\mu\text{s}$ , leading us to conclude that the prepared metal complex was an electrolyte. Silver nitrate solution was used as an indicator for the determination of chloride ions, showing that the chloride ions were not linked with metal ions in the coordination sphere. Metallic calculations indicated that the complex was monometallic. The structural formula of the complex is shown in fig. 3.

**Synthesis of  $[\text{Ni}(\text{TMADPH})\text{Cl}_2]$  complex:** 0.188 g, 0.5 mmol was dissolved in 20 ml of methanol in a clean two-necked round bottom flask (250 mL) equipped with a magnetic stirrer and reflux condenser.  $\text{NiCl}_2$  (0.065 g, 0.5mmol) was added drop by drop to the ligand solution. The pH was adjusted to 11 using KOH and the mixture was then stirred at 65°C for 12 hours. The resulting precipitate was filtered, washed with methanol and then diethyl ether, dried and weighed. The melting point was determined as >300°C. Electrical conductivity was measured for the metal complexes and it was 25.8  $\mu\text{s}$ , leading us to conclude that the prepared metal complex was an electrolyte. Silver nitrate solution was used as an indicator for the determination of chloride ions, showing that the chloride ions were linked with metal ions in the coordination sphere. Metallic calculations indicated that the complex was monometallic. The structural formula of the complex is shown in fig. 4.

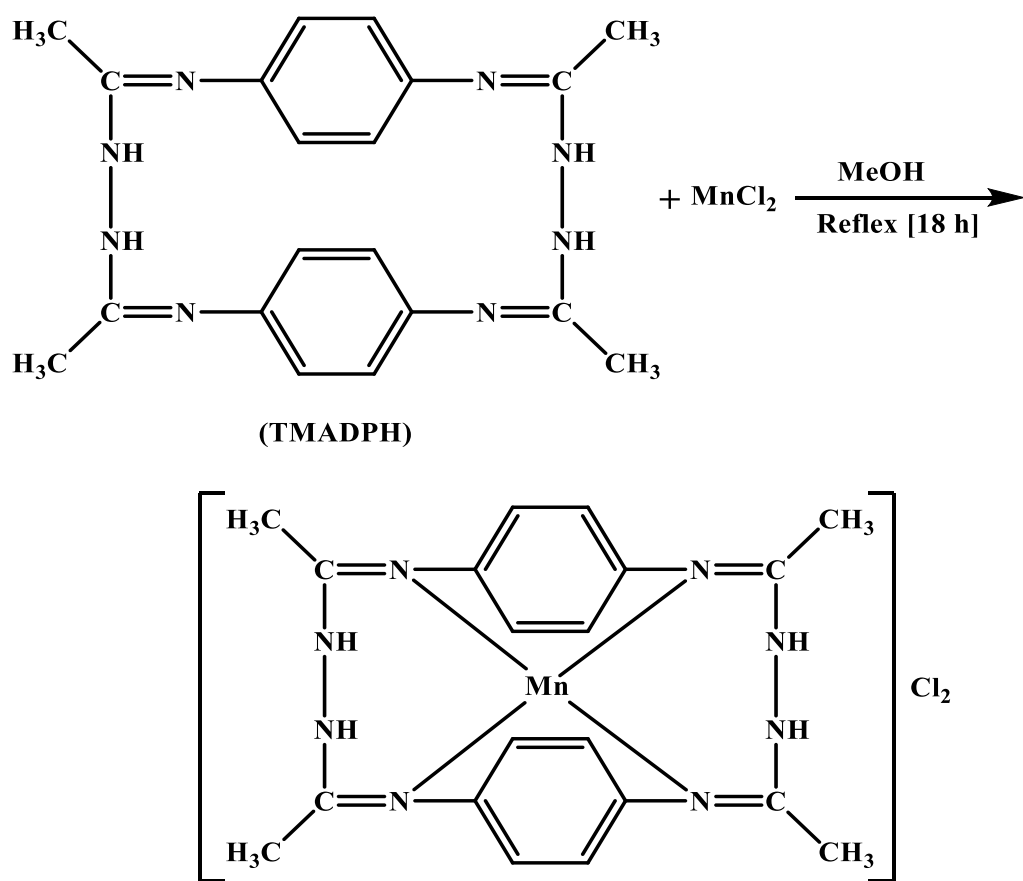


Fig. 3: The structural formula of the metal complex

Table 1  
The physical properties of the prepared compounds

Comp.	Formula	M (g.mol <sup>-1</sup> )	Color	Melting point °C	Yield (%)
TMADPH	$\text{C}_{20}\text{H}_{24}\text{N}_8$	376.4572	Brown	180	56.732
$[\text{Zr}(\text{TMADPH})\text{Cl}_2]\cdot\text{Cl}_2$	$\text{C}_{20}\text{H}_{24}\text{Cl}_4\text{N}_8\text{Zr}$	609.4932	Dark Brown	>300	63.157
$[\text{Mn}(\text{TMADPH})]\cdot\text{Cl}_2$	$\text{C}_{20}\text{H}_{24}\text{Cl}_2\text{N}_8\text{Mn}$	502.31	Dark Brown	>300	56.800
$[\text{Ni}(\text{TMADPH})\text{Cl}_2]$	$\text{C}_{20}\text{H}_{24}\text{Cl}_2\text{N}_8\text{Ni}$	506.06	Dark Brown	>300	84.126

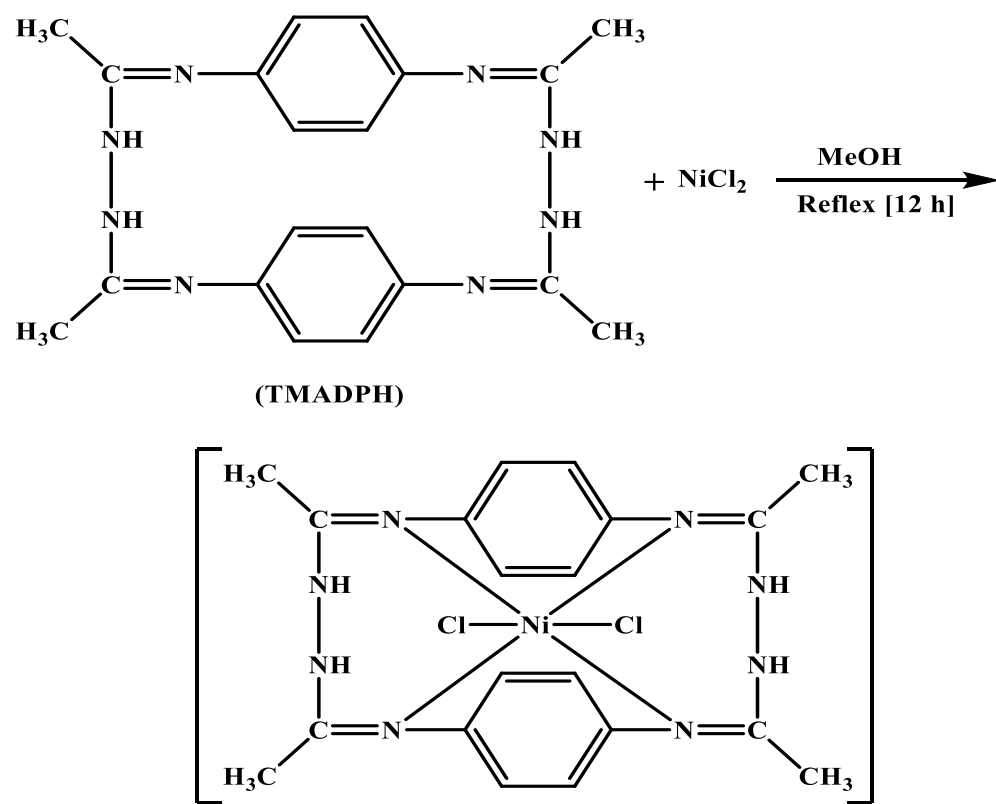
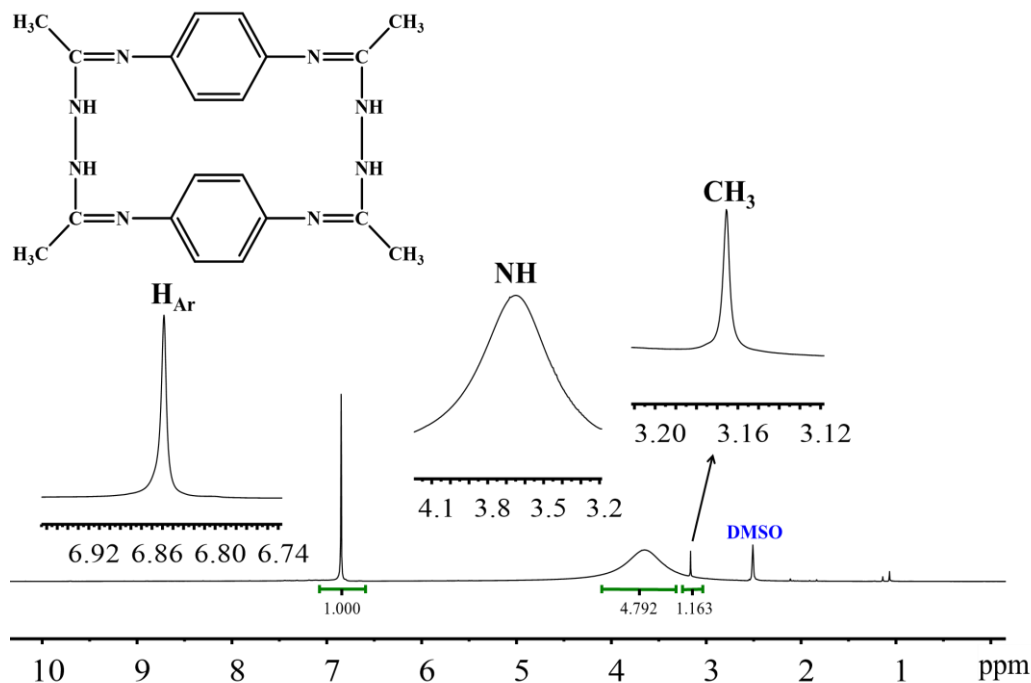


Fig. 4: The structural formula of the metal complex.

Fig. 5:  $^1\text{H}$  NMR spectrum of TMADPH

## Results and Discussion

**NMR characterization:** TMADPH compounds were characterized using  $^1\text{H}$ -NMR,  $^{13}\text{C}$ -NMR as follow: The  $^1\text{H}$ -NMR spectrum of the ligand (TMADPH) showed no signal corresponding to primary amine protons. This suggests the derivatization of carbonyl groups:  $^1\text{H}$  NMR (400 MHz, DMSO)  $\delta$  3.1 ppm (S, 12H), 3.63 ppm (S, 4H),  $\delta$  6.83 ppm

(S, 8H).  $^{13}\text{C}$  NMR (125 MHz, DMSO):  $\delta$  25.37, 119.42, 134.39, 168.76 ppm.

**FT-IR of TMADPH ligand and its complexes:** The IR spectrum of the free ligand exhibited no bands corresponding to the free primary diamine or a free keto group. This suggests complete condensation of the amino

groups with the keto groups. The bands at 1636 and 1615  $\text{cm}^{-1}$  are due to  $\nu(\text{C}=\text{N})$  vibrations of the azomethine. The bands at 3326  $\text{cm}^{-1}$  belongs to N–H. The strong and sharp absorption bands appearing in the regions 2925–3010 and 1385  $\text{cm}^{-1}$  in the spectra of all complexes may be due to  $\text{CH}_3$  stretching and bending vibrations respectively. The bands at 1505  $\text{cm}^{-1}$  belong to C=C. The bands at 1568  $\text{cm}^{-1}$  belongs

to C–N–H and the bands at 3414  $\text{cm}^{-1}$  belongs to C<sub>aromatic</sub>–N<sup>8</sup>. On complexation, the position of the  $\nu(\text{C}=\text{N})$  band shifted by 9–14  $\text{cm}^{-1}$  to lower wavenumbers, indicating coordination through the N atoms of the imine groups. The most important IR data of the TMADPH ligand and its complexes are summarized in table 2.

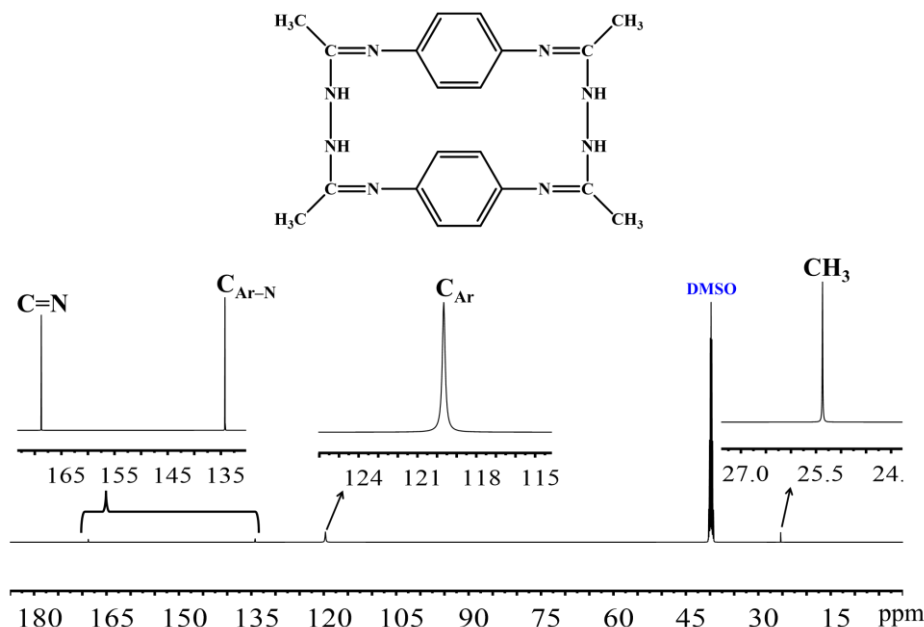


Fig. 6:  $^{13}\text{C}$  NMR spectrum of TMADPH

Table 2  
The absorption bands of TMADPH and its complexes

Comp.	$\text{C}_{\text{aromatic}}-\text{N}$ $\bar{\nu}, \text{cm}^{-1}$	$\text{N}-\text{H}$ $\bar{\nu}, \text{cm}^{-1}$	$\text{C}=\text{N}$ $\bar{\nu}, \text{cm}^{-1}$	$\text{C}=\text{C}$ $\bar{\nu}, \text{cm}^{-1}$	$\text{C}-\text{N}-\text{H}$ $\bar{\nu}, \text{cm}^{-1}$	$\text{CH}_3$ (bend) $\bar{\nu}, \text{cm}^{-1}$
TMADPH	3414	3326	1636 1615	1505	1586	1385
$[\text{Zr}(\text{TMADPH})\text{Cl}_2]\cdot\text{Cl}_2$	3342	3203	1625 1606	1510	1573	1384
$[\text{Mn}(\text{TMADPH})]\cdot\text{Cl}_2$	3325	3176	1627 1605	1510	-	1384
$[\text{Ni}(\text{TMADPH})\text{Cl}_2]$	-----	3419	1624 1606	1508	-	-

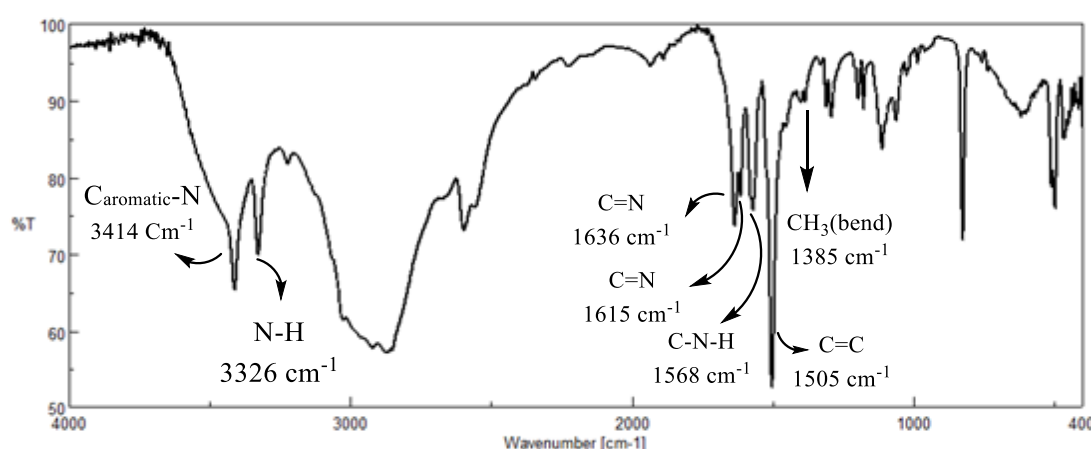


Fig. 7: FT-IR spectrum of TMADPH.

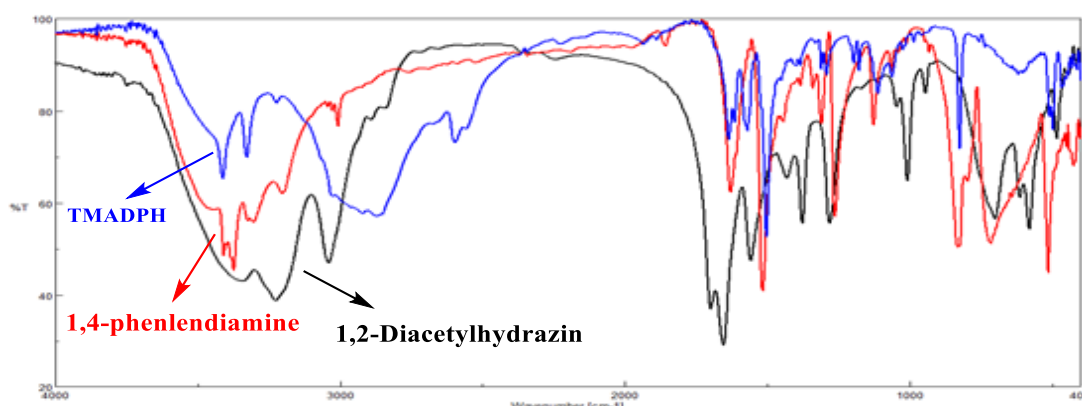


Fig. 8: FT-IR spectrum of TMADPH compared with 1, 2-Diacetylhydrazin and 1,4 –Phenylendiamine.

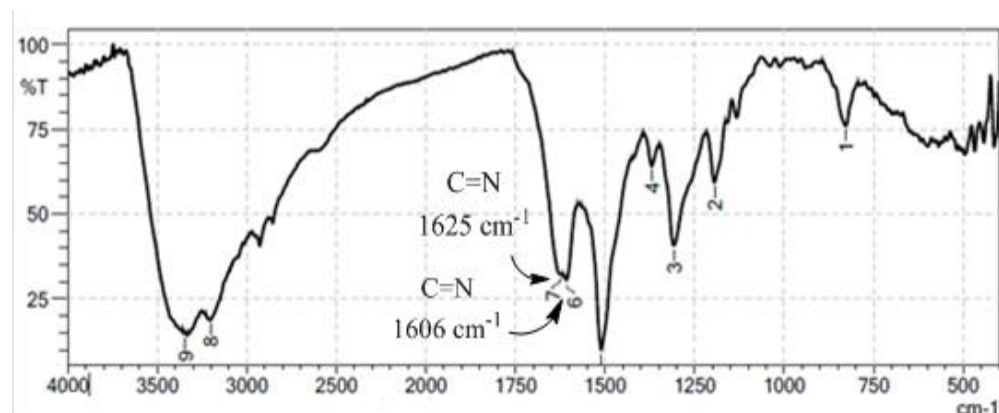


Fig. 9: FT-IR spectrum of  $[\text{Zr}(\text{TMADPH})\text{Cl}_2] \cdot \text{Cl}_2$

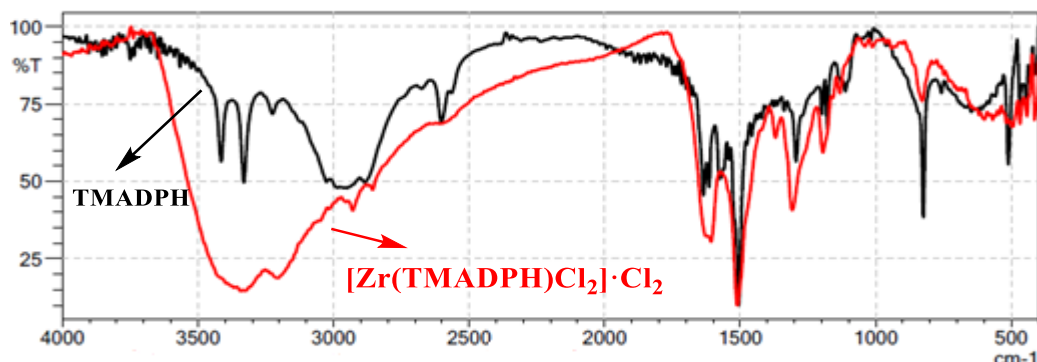


Fig. 10: FT-IR spectrum of  $[\text{Zr}(\text{TMADPH})\text{Cl}_2] \cdot \text{Cl}_2$  Compared with TMADPH.

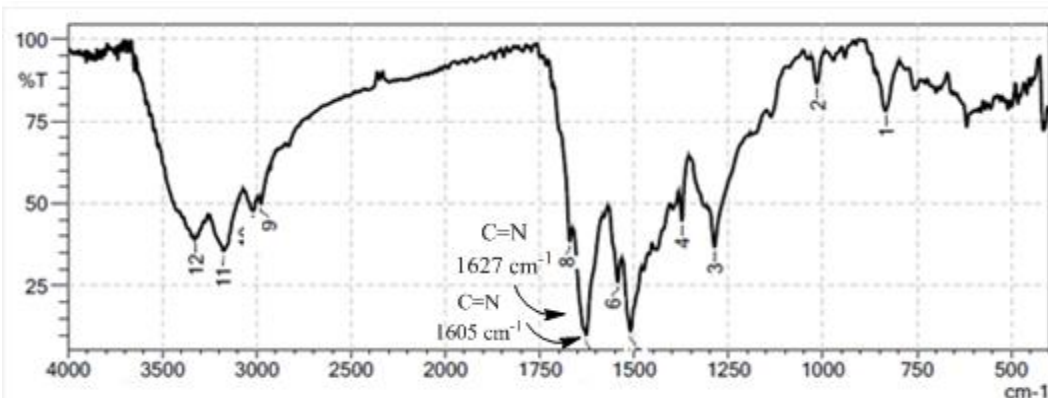


Fig. 11: FT-IR spectrum of  $[\text{Mn}(\text{TMADPH})] \cdot \text{Cl}_2$ .

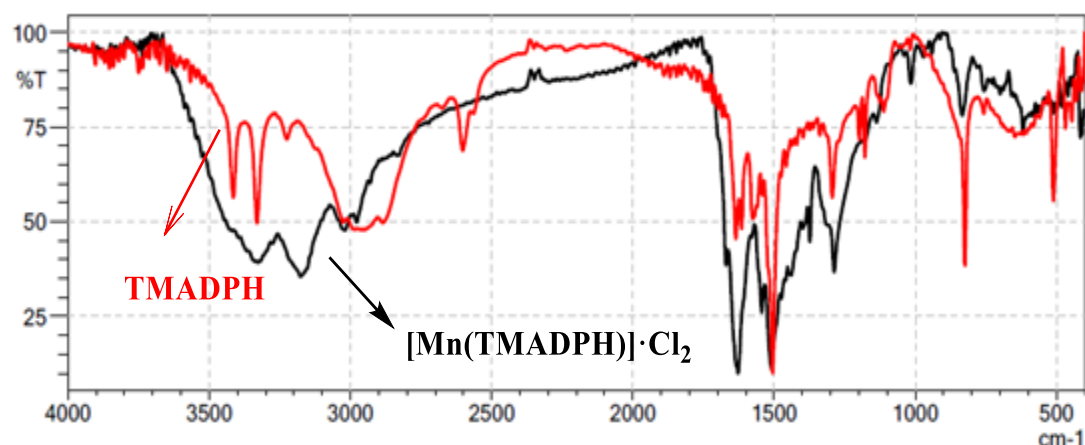
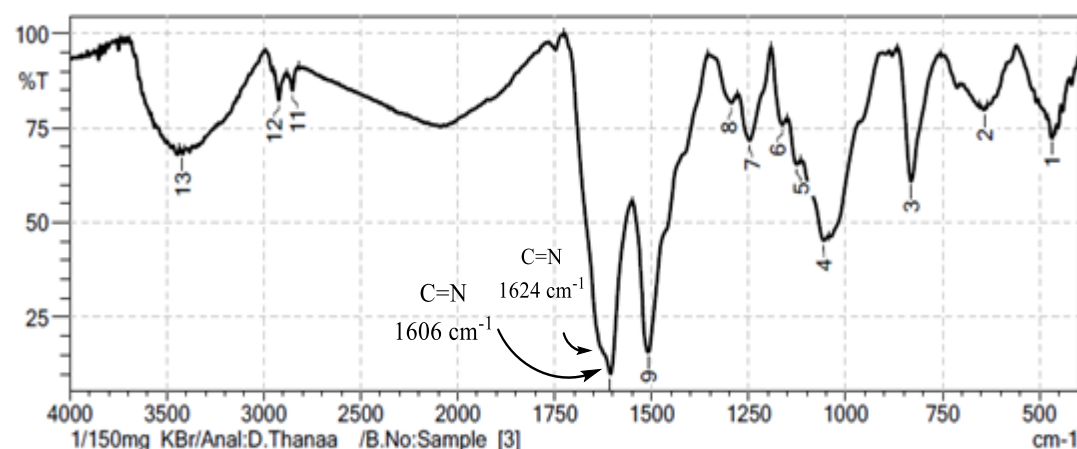
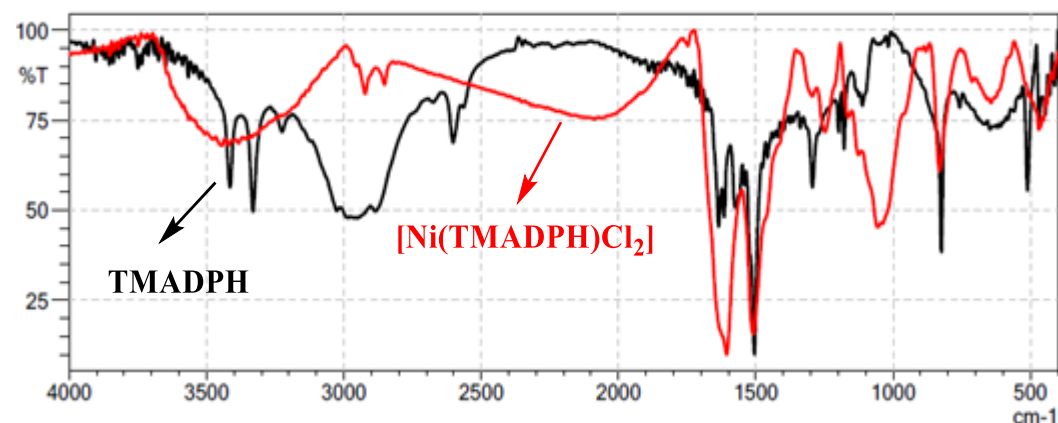
Fig. 12: FT-IR spectrum of  $[\text{Mn}(\text{TMADPH})]\cdot\text{Cl}_2$  Compared with TMADPHFig. 13: FT-IR spectrum of  $[\text{Ni}(\text{TMADPH})\text{Cl}_2]$ .Fig. 14: FT-IR spectrum  $[\text{Ni}(\text{TMADPH})\text{Cl}_2]$  Compared with TMADPH

Table 3  
The electronic transitions for TMADEH and their complexes.

Comp.	$\pi \rightarrow \pi^*$	$n \rightarrow \pi^*$	$d-d$	$L-M$
TMADPH	264 nm	300 nm	-----	
$[\text{Zr}(\text{TMADPH})\text{Cl}_2]\cdot\text{Cl}$	264 nm	320 nm		580 nm
$[\text{Mn}(\text{TMADPH})]\cdot\text{Cl}_2$	264 nm	290 nm	500 nm	
$[\text{Ni}(\text{TMADPH})\text{Cl}_2]$	264 nm	-----	528 nm	

**UV-Vis characterization:** The electronic spectra of the TMADPH ligand and its complexes show the electronic transitions between energy levels. Figures (15 to 19) present the UV-Vis spectra of TMADPH ligand and its complexes.

**Elemental analysis for ligand:** The macrocyclic ligand was subjected to elemental analyses. The results of the elemental analyses (C, H and N) of the ligand are given in Table 4.

**Antibacterial Activity Study:** The antibacterial efficacy of the prepared compounds was tested against *Pseudomonas aeruginosa* and *Staphylococcus aureus* bacteria, using gentamicin as a reference. Two different concentrations (50 and 100 mg/ml) of the compounds and gentamicin were selected for the antibacterial assay.

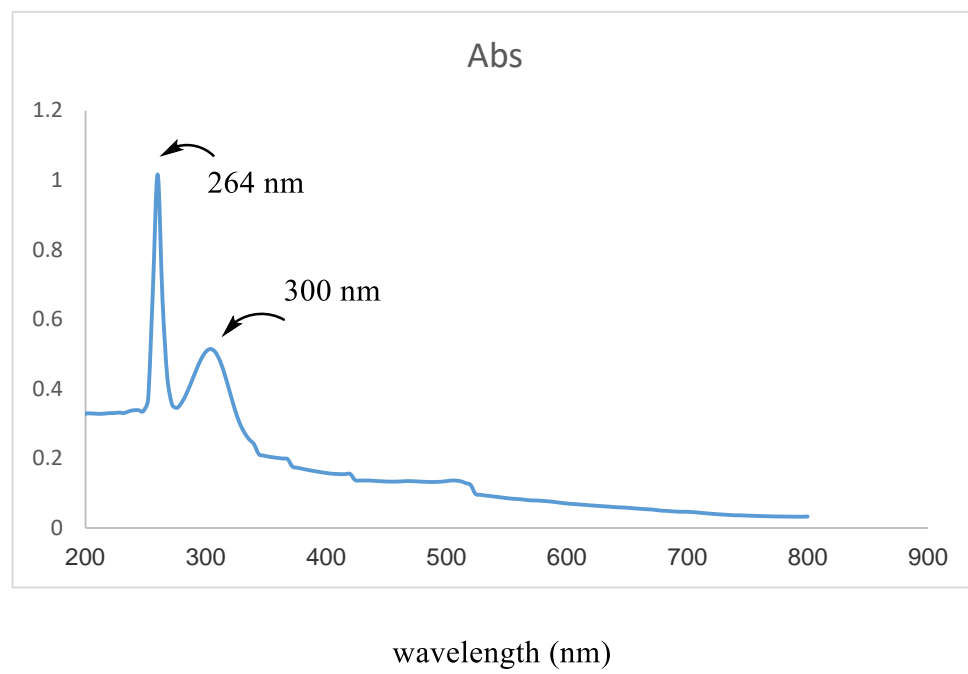


Fig. 15: UV-Vis spectrum of TMADPH.

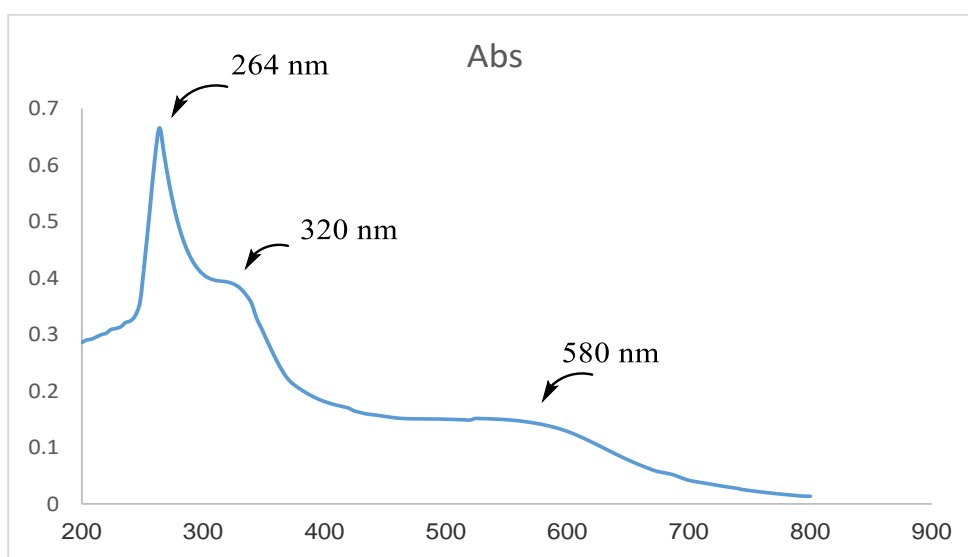
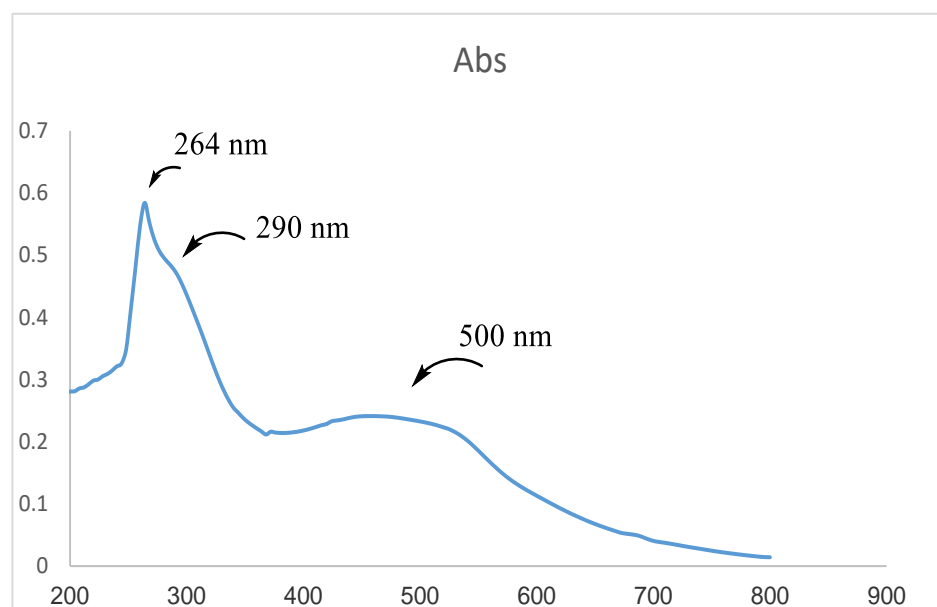
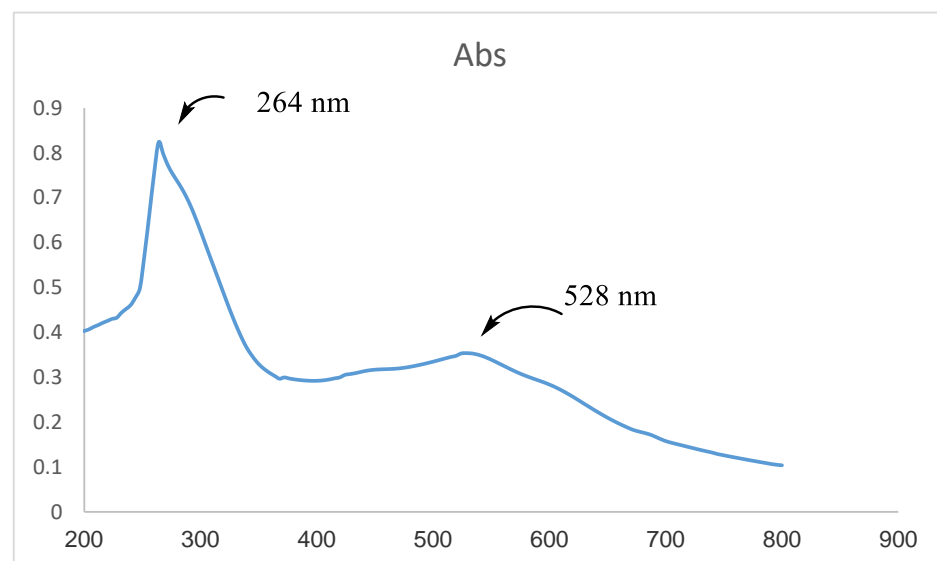


Fig. 16: UV-Vis spectrum of  $[\text{Zr}(\text{TMADPH})\text{Cl}_2]\cdot\text{Cl}$

Table 4  
The Elemental analysis for TMADEH.

Comp.	$\text{C}_{20}\text{H}_{24}\text{N}_8$	
	Calculated %	Found %
C	63.50	63.80
H	6.41	6.42
N	29.75	29.76

Fig. 17: UV-Vis spectrum of  $[\text{Mn(TMADPH)}] \cdot \text{Cl}_2$ .Fig. 18: UV-Vis spectrum of  $[\text{Ni(TMADPH)}\text{Cl}_2]$ 

**Table 5**  
Biological test results of the *P. aeruginosa* and *S. aureus*

	50 ( $\mu\text{g/mL}$ )		100 ( $\mu\text{g/mL}$ )	
	<i>Staphylococcus aureus</i> (+)	<i>Pseudomonas aeruginosa</i> (-)	<i>Staphylococcus aureus</i> (+)	<i>Pseudomonas aeruginosa</i> (-)
Gentamicine	23	23	27	24
DMSO	0	0	0	0
TMADPH	13	12	13	14
$[\text{Mn(TMADPH)}] \cdot \text{Cl}_2$	15	14	13	16

In our research, we chose to study *P. aeruginosa* and *S. aureus* bacteria because of their widespread presence in society, impacting daily human life. *P. aeruginosa* is a type of bacteria commonly found in the environment, such as soil and water. Among the various types of *Pseudomonas*, *Pseudomonas aeruginosa* is the most common cause of

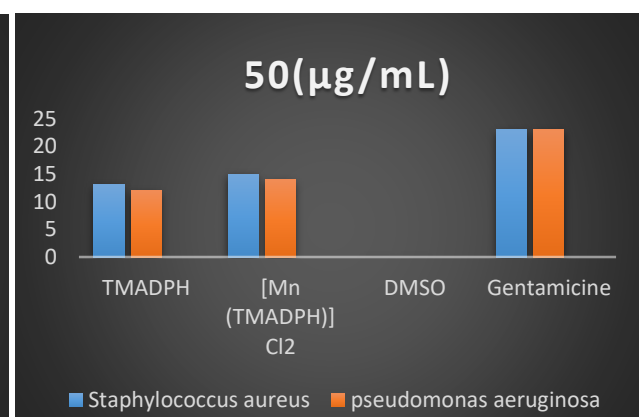
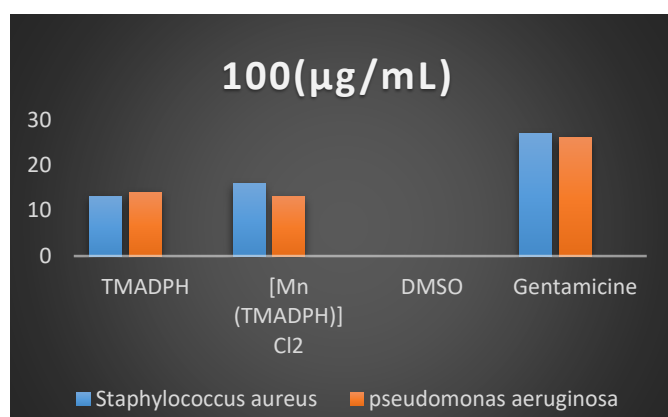
infections in humans, leading to conditions such as bloodstream and lung infections (pneumonia), or infections in other parts of the body after surgery<sup>15</sup>. *Staphylococcus aureus* is a significant bacterial pathogen in humans, responsible for a diverse range of clinical symptoms<sup>1</sup>. The results are arranged in the table 5.



**Fig. 19: Inhibition zone at different concentration against Gram-positive and Gram-negative to (TMADPH)**



**Fig. 20: Inhibition zone at different concentration against Gram-positive and Gram-negative to [Mn (TMADPH)]Cl<sub>2</sub>**



**The graphical presentation of the antibacterial activity against tested bacteria at (50 µg/mL) and (100 µg/mL)**

## Conclusion

In summary, a new macrocyclic ligand and its metal complexes were successfully prepared and characterized using <sup>1</sup>H-NMR, <sup>13</sup>C-NMR, UV-Vis, FT-IR. The results indicate a mononuclear structure in the metal complexes. The biological activity against *Pseudomonas aeruginosa* and *Staphylococcus aureus* bacteria was studied. It was found that the prepared metal complexes have higher biological activity than Schiff base ligands, which promised amazing results for the prepared compounds in various pharmacological applications.

## References

- Buck J.M., Como-Sabetti K., Harriman K.H., Danila R.N., Boxrud D.J., Glennen A. and Lynfield R., Community-associated methicillin-resistant *Staphylococcus aureus*, Minnesota, 2000–2003, *Emerging Infectious Diseases*, **11**(10), 1532 (2005)
- Chandra S., Tyagi M., Rani S. and Kumar S., Lanthanide complexes derived from hexadentate macrocyclic ligand: Synthesis, spectroscopic and thermal investigation,

*Spectrochimica Acta Part A: Molecular and Biomolecular Spectroscopy*, **75**(2), 835-40 (2010)

- Chandra S., Tyagi M. and Sharma K., Mn (II), Co (II), Ni (II) and Cu (II) complexes of a tertraaza macrocyclic ligand: Synthesis, characterization and biological screening, *Journal of the Iranian Chemical Society*, **6**(2), 310-316 (2009)
- Chandra S. and Verma S., Spectroscopic studies of transition metal complexes with a N-donor tetradentate (N4) 12-membered macrocyclic ligand, *Spectrochimica Acta Part A: Molecular and Biomolecular Spectroscopy*, **71**(2), 458-464 (2008)
- Driggers E.M., Hale S.P., Lee J. and Terrett N.K., The exploration of macrocycles for drug discovery—an underexploited structural class, *Nature Reviews Drug Discovery*, **7**(7), 608-624 (2008)
- Ferraudi G., Canales J.C., Kharisov B., Costamagna J., Zagal J.G., Cardenas-Jiron G. and Paez M., Synthetic N-substituted metal aza-macrocyclic complexes: properties and applications, *Journal of Coordination Chemistry*, **58**(1), 89-109 (2005)

7. Ilhan S., Temel H., Yilmaz I. and Sekerci M., Synthesis and characterization of new macrocyclic Schiff base derived from 2, 6-diaminopyridine and 1, 7-bis (2-formylphenyl)-1, 4, 7-trioxaheptane and its Cu (II), Ni (II), Pb (II), Co (III) and La (III) complexes, *Polyhedron*, **26**(12), 2795-802 (2007)

8. Iqbal M.A., Haque R.A., Ahamed M.B., Majid A.A. and Al-Rawi S.S., Synthesis and anticancer activity of para-xylyl linked bis-benzimidazolium salts and respective Ag (I) N-heterocyclic carbene complexes, *Medicinal Chemistry Research*, **22**(5), 2455-2466 (2013)

9. Khue Thi Nguyen, Nguyen Thi Thu Hien, Le Thi Thanh Huyen, Roan Thi Do and Huong Thi Thanh Doan, Molecular characterization of Marek's disease virus revealing the predominance of high-virulence MDV in Vietnam, *Res. J. Biotech.*, **18**(11), 70-80 (2023)

10. Kumar R. and Singh R., Chromium (III) complexes with different chromospheres macrocyclic ligands: synthesis and spectroscopic studies, *Turkish Journal of Chemistry*, **30**(1), 77-87 (2006)

11. Krahn D., Ottmann C. and Kaiser M., Macrocyclic proteasome inhibitors, *Current Medicinal Chemistry*, **18**(33), 5052-5060 (2012)

12. Mandal L., Sasmal S., Sparkes H.A., Howard J.A. and Mohanta S., Crystal structure, catecholase activity and ESI-MS of a mixed valence cobalt (III)-cobalt (II) complex derived from a macrocyclic ligand: Identification/proposition of hydrogen bonded metal complex solvent aggregates in ESI-MS, *Inorganica Chimica Acta*, **412**, 38-45 (2014)

13. Mallinson J. and Collins I., Macrocycles in new drug discovery, *Future Medicinal Chemistry*, **4**(11), 1409-1438 (2012)

14. Meyer F. and Kozlowski H., Comprehensive Coordination Chemistry II, McCleverty J.A. and Meyer T.J., Eds. (2004)

15. Qin S., Xiao W., Zhou C., Pu Q., Deng X., Lan L. and Wu M., Pseudomonas aeruginosa: pathogenesis, virulence factors, antibiotic resistance, interaction with host, technology advances and emerging therapeutics, *Signal Transduction and Targeted Therapy*, **7**(1), 199 (2022)

16. Rani S., Kumar S. and Chandra S., Synthesis of nnnn tetradeятate macrocyclic ligand and its Pd (II), Pt (II), Ru (III) and Ir (III) complexes: Spectroscopic, thermal and antimicrobial studies, *Synthesis and Reactivity in Inorganic, Metal-Organic and Nano-Metal Chemistry*, **40**(10), 940-946 (2010)

17. Singh D.P., Kumar R., Malik V. and Kumar K., One pot template synthesis and characterization of trivalent transition metal ion complexes derived from diaminopyridine and glyoxal, *Rasayan Journal of Chemistry*, **1**(2), 349-354 (2008)

18. Shimakoshi H., Nakazato A., Hayashi T., Tachi Y., Naruta Y. and Hisaeda Y., Electroorganic syntheses of macrocyclic lactones mediated by vitamin B12 model complexes: Part 17, Hydrophobic vitamin B12, *Journal of Electroanalytical Chemistry*, **507**(1-2), 170- 176 (2001).

(Received 07<sup>th</sup> September 2024, accepted 15<sup>th</sup> November 2024)